Clim Dyn (2017) 49:1321–1339
DOI 10.1007/s00382-016-3389-8

Linking a sea level pressure anomaly dipole over North America to the central Pacific El Niño

Ruiqiang Ding[1,2] · **Jianping Li**[3,4] · **Yu-heng Tseng**[5] · **Cheng Sun**[3,4] · **Fei Zheng**[1]

Received: 7 January 2016 / Accepted: 6 October 2016 / Published online: 12 October 2016

Abstract This study demonstrates the close connection between the north–south dipole pattern of sea level pressure anomalies over northeastern North America to the western tropical North Atlantic, referred to as the North American dipole (NAD), and the central Pacific (CP)-type El Niño a year later. In contrast to other ENSO precursors, such as the North Pacific Oscillation (NPO) and Pacific–North America (PNA) pattern, the NAD appears more closely related to the CP-type El Niño than to the eastern Pacific (EP)-type El Niño, indicating that the NAD may serve as a unique precursor for the CP El Niño. The wintertime NAD induces sea surface temperature anomalies in the northern tropical Atlantic (NTA), which subsequently play an important role in developing the CP El Niño-like pattern in the tropical Pacific over the course of the following year. It appears that the NAD influence on CP El Niño involves air–sea interaction over several major basins, including the subtropical/tropical Pacific and the NTA. Additional analysis indicates that the correlation of either the NAD index or the NPO index with the CP El Niño state a year later depends on the status of the other index. When the wintertime NAD index is of the opposite sign to the simultaneous NPO index, the correlation of the NAD or NPO index with the Niño4 index becomes much weaker.

Keywords Central Pacific El Niño · North American dipole (NAD) · North Pacific Oscillation (NPO)

1 Introduction

The El Niño-Southern Oscillation (ENSO) phenomenon, which originates in the tropical Pacific, is the strongest natural interannual climate signal and has received much attention because of both its worldwide climatic and economic effects. It has been increasingly recognized that there are two different flavors or types of El Niño events in the tropical Pacific. The new type of El Niño is known as the Central Pacific El Niño (CP El Niño; Yu and Kao 2007; Kao and Yu 2009), which exhibits maximum positive sea surface temperature (SST) anomalies in the central equatorial Pacific, rather than the eastern equatorial Pacific as seen during conventional El Niño episodes (referred to as the Eastern Pacific (EP) El Niño). Different terms have also been used to describe the CP El Niño, including the Date Line El Niño (Larkin and Harrison 2005), El Niño Modoki (Ashok et al. 2007), and warm-pool El Niño (Kug et al. 2009). There is increasing observational and modeling evidence that the two types of El Niño events result from different dynamical processes (Ashok and Yamagata 2009; Kao and Yu 2009; Kug et al. 2009) and that they have markedly different impacts on the weather and climate around the world (e.g., Taschetto and England 2009; Feng

✉ Ruiqiang Ding
drq@mail.iap.ac.cn

1 State Key Laboratory of Numerical Modeling for Atmospheric Sciences and Geophysical Fluid Dynamics (LASG), Institute of Atmospheric Physics, Chinese Academy of Sciences, Beijing 100029, China

2 Plateau Atmosphere and Environment Key Laboratory of Sichuan Province, Chengdu University of Information Technology, Chengdu 610225, China

3 College of Global Change and Earth System Sciences (GCESS), Beijing Normal University, Beijing 100875, China

4 Joint Center for Global Change Studies, Beijing 100875, China

5 Climate and Global Dynamics Division, NCAR, Boulder, CO, USA

and Li 2011; Weng et al. 2011; Gushchina and Dewitte 2012; Wilson et al. 2014; Zhang et al. 2015).

Previous studies have suggested that the North Pacific Oscillation (NPO; Walker and Bliss 1932; Rogers 1981), the second leading mode of sea level pressure (SLP) anomalies over the North Pacific, can influence the occurrence of ENSO events (Vimont et al. 2001, 2003a, b; Anderson 2003; Alexander et al. 2010; Yu and Kim 2011). The seasonal footprinting mechanism (SFM) has been proposed by Vimont et al. (2001, 2003a, b) to explain how NPO-like atmospheric variability could lead to tropical SST variability. The SFM suggests that fluctuations in the wintertime NPO impart an SST footprint onto the ocean via changes in the net surface heat flux. This SST footprint, which is termed the Victoria mode (VM; Bond et al. 2003; Ding et al. 2015a, b) or Pacific Meridional Mode (PMM; Chiang and Vimont 2004; Chang et al. 2007), peaks in late winter and early spring, and persists until summer via atmosphere–ocean coupling in the subtropics. In this region, the SST anomalies can subsequently force the overlying atmosphere, resulting in anomalous zonal wind stress across the equatorial Pacific that is conducive to initiating an ENSO event during the following winter. In addition to the SFM, the NPO influence on ENSO may occur through the "trade wind charging mechanism (TWC)" whereby subsurface temperature anomalies across the central equatorial Pacific resulting from the NPO-induced variations in the trade winds can subsequently favor the development of an ENSO event (Anderson et al. 2013). The connection between the NPO and ENSO a year later indicates that the NPO may be a reliable precursor signal for ENSO events, which has important implications for prediction of ENSO variability (Vimont et al. 2003a).

Given that there are two distinct types of El Niño, the question naturally arises as to whether the NPO-like extratropical atmospheric forcing is more likely to induce a particular type of El Niño (i.e., the CP or EP El Niño). Some studies have indicated that the NPO and its associated SST footprint (i.e., the VM or PMM pattern) play a particularly important role in exciting the CP El Niño (Yu et al. 2010, 2012; Yu and Kim 2011; Kim et al. 2012; Lin et al. 2015). However, other analyses also have found no strong evidence that the NPO and its associated SST footprint tend to be more conducive to the initialization of the CP El Niño than the EP El Niño (Pegion and Alexander 2013; Ding et al. 2015a). An early study by Vimont et al. (2003a) indicated that the NPO is followed by a typical EP El Niño pattern (see their Figs. 1 and 3). Larson and Kirtman (2014) reported that the strong 1997–1998 El Niño (a typical EP El Niño event) is preceded by a positive PMM anomaly. Alexander et al. (2010) reported that equatorial ocean dynamics, such as the zonal advection in the tropical Pacific, can extend the NPO-induced warming in the central Pacific eastwards, leading to EP El Niño events. A recent study by Ding et al. (2015a) reported that although the NPO and its associated SST footprint may trigger the initial warming

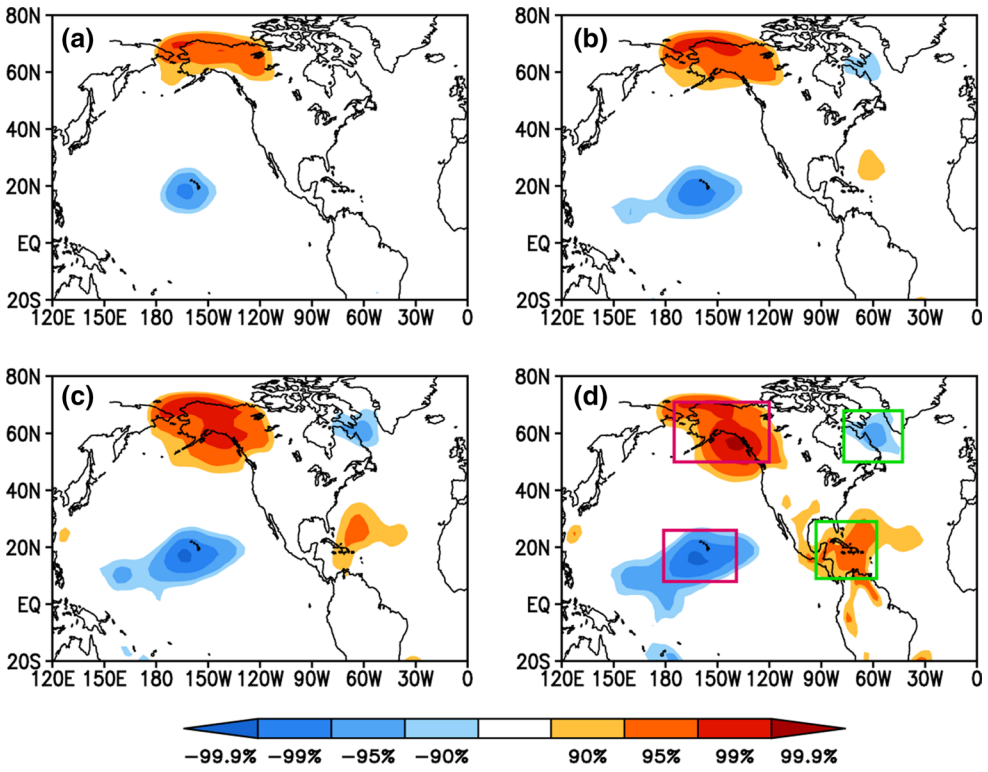

Fig. 1 Correlation maps of winter [November–March (NDJFM)] averaged **a** Niño1+2, **b** Niño3, **c** Niño3.4, and **d** Niño4 indices correlated with SLP anomalies a year earlier for the period 1979–2013. In **a**–**d**, areas with a correlation significant at or above the 90 % confidence level are *shaded*. In **d**, the *two magenta boxes* indicate the locations of the northern (175–120°W, 50–71°N) and southern (179°E–139°W, 8–26°N) poles of the NPO, and the *two green boxes* indicate the locations of the southern (93–58°W, 9–29°N) and northern (77–43°W, 53–68°N) poles of the NAD

in the central equatorial Pacific, the latter could finally develop respectively to the CP El Niño and EP El Niño patterns, possibly depending on equatorial ocean dynamics as suggested by Alexander et al. (2010). They further showed that two CP El Niño events (1986/1987 and 1991/1992) and also two EP El Niño events (1982/1983 and 1997/1998) were preceded by the NPO signature. Capotondi and Sardeshmukh (2015) and Capotondi et al. (2015) suggested that different SST precursors (including the PMM) alone do not favor the generation of different ENSO types, and instead the initial thermocline state of the equatorial Pacific may play an important distinguishing role in the development of the CP or EP El Niño events. These findings indicate that if we rely on the wintertime NPO precursor signal alone, we cannot judge in advance whether the NPO is more likely to be followed by an EP El Niño or a CP El Niño event. Therefore, it is necessary to further examine the differences between the atmospheric precursor signals of the two types of El Niño events, and to identify an additional precursor signal that is more conducive to initiating the CP El Niño than the EP El Niño, or vice versa. We believe that identifying such a precursor for the CP El Niño alone (or for the EP El Niño alone) would greatly improve ENSO prediction and also enhance seasonal climate prediction, as the CP El Niño is thought to produce different climate impacts than the EP El Niño (e.g., Taschetto and England 2009; Feng and Li 2011; Weng et al. 2011; Gushchina and Dewitte 2012; Wilson et al. 2014; Zhang et al. 2015).

The focus of this paper is the search for a precursor signal associated with the atmospheric variability that precedes ENSO events, which is not only distinct from the NPO, but may also act as a potential predictor of the type of El Niño event that will be generated. The remainder of this paper is organized as follows. Section 2 describes the various datasets used in this study. Section 3 investigates the differences between the SLP patterns preceding CP and EP El Niño events, and identifies a precursor SLP signal that is more closely linked to the CP El Niño than to the EP El Niño. This section also discusses the possible mechanisms linking the precursor SLP signal to the CP El Niño, and the joint relationship of this precursor SLP signal and NPO to the CP El Niño. Our findings are summarized and discussed in Sect. 4.

2 Data

We used the monthly mean SST field from the National Oceanic and Atmospheric Administration (NOAA) Extended Reconstructed SST version 3b dataset (ERSSTv3b; Smith et al. 2008). The ERSSTv3b dataset has a horizontal resolution of 2° × 2° and runs from 1854 to the present. We used the monthly mean subsurface ocean temperature from the Simple Ocean Data Assimilation (SODA) reanalysis for the period 1871–2010 (Giese and Ray 2011). The SODA dataset has 23 vertical levels unevenly distributed from 5 to 1139 m, and covers the global oceans from 30.75°S to 30.75°N with a horizontal resolution of 0.5° × 0.5°. We used atmospheric fields from the National Centers for Environmental Prediction–National Center for Atmospheric Research (NCEP–NCAR) reanalysis data on a 2.5° × 2.5° grid (Kalnay et al. 1996). We used the precipitation field from the Climate Prediction Center (CPC) Merged Analysis of Precipitation (CMAP) dataset (Xie and Arkin 1997). The CMAP dataset contain monthly precipitation data (mm day^{-1}) at a spatial resolution of 2.5° × 2.5°. In all calculations based on monthly mean data, the monthly anomalies were calculated by removing the climatological monthly means.

The Pacific–North America (PNA) teleconnection pattern is one of the most prominent modes of low-frequency atmospheric variability in the Northern Hemisphere extratropics (Horel and Wallace 1981; Wallace and Gutzler 1981). The PNA index is determined using the modified pointwise method (described online at http://www.cpc.ncep.noaa.gov/products/precip/CWlink/pna/month_pna_index2.shtml; the index values are available online at this website), which is based on the pointwise method of Wallace and Gutzler (1981). The North Atlantic Oscillation (NAO) is the dominant mode of atmospheric variability over the North Atlantic region (Barnston and Livezey 1987; Hurrell 1995). The NAO index is defined as the difference in the normalized SLP regionally zonal-averaged over the North Atlantic sector from 80°W to 30°E between 35°N and 65°N (Li and Wang 2003). Note that our analysis was focused mainly on the period 1979–2013, because the precipitation, NCEP–NCAR reanalysis, SST, and subsurface ocean temperature data were all available for this timespan. However, in Sect. 4 we also use longer datasets (back to 1950) to investigate the decadal variations in the relationship between the CP El Niño and its precursor SLP signal.

3 Results

3.1 Difference between the SLP patterns preceding CP and EP El Niño

Four regional indices are currently used to monitor ENSO: Niño1+2 (90–80°W, 10°S–0°), Niño3 (150–90°W, 5°S–5°N), Niño3.4 (170–120°W, 5°S–5°N), and Niño4 (160°E–150°W, 5°S–5°N). Among them, the Niño3 index is commonly used to measure the intensity of EP El Niño events, whereas the Niño4 index is commonly used to measure the intensity of CP El Niño events (Kug et al. 2009).

Table 1 Correlations of the winter (NDJFM) averaged NPO and NAD indices with the four NINO indices a year later for the period 1979–2013

	Niño1+2	Niño3	Niño3.4	Niño4
NPO	0.42*	0.51**	0.58**	0.59**
NAD	0.15	0.27	0.38*	0.44*

* Statistically significant correlation significant at the 95 % confidence level

** Statistically significant correlation significant at the 99 % confidence level

Figure 1a–d show the spatial patterns of winter [November–March (NDJFM)] averaged Niño1+2, Niño3, Niño3.4, and Niño4 indices correlated with SLP anomalies a year earlier for the period 1979–2013. All four indices are preceded, by one year, by an NPO-like pattern over the North Pacific, and this is consistent with previous findings (Vimont et al. 2001, 2003a, b; Anderson 2003; Alexander et al. 2010; Yu and Kim 2011). In comparison, the NPO-like patterns preceding the Niño3.4 index, and preceding the Niño4 index, are very similar, both of which appear to be slightly more pronounced than the pattern preceding the Niño3 index, with a larger domain of significant correlations over both the northern and southern poles of the NPO. The NPO-like pattern preceding the Niño1+2 index is still visible, but is weaker than those preceding other ENSO indices (including the Niño3, Niño3.4, and Niño4 indices).

We then calculated the correlation coefficients between the NDJFM-averaged NPO index and the four NINO indices a year later (Table 1). The NPO index is defined here as the difference between the normalized SLP anomalies averaged over the northern (175–120°W, 50–71°N) and southern (179°E–139°W, 8–26°N) poles (indicated by the magenta boxes in Fig. 1d). All of the correlations are significant at or above the 95 % confidence level. The correlation coefficient between the Niño1+2 index and the NPO index from the previous winter is 0.42. Moving west from the eastern to the central Pacific, the correlation coefficients associated with the relationships between the Niño3, Niño3.4, and Niño4 indices and the NPO index from the previous winter are 0.51, 0.58, and 0.59, respectively. The differences between these correlations are generally small and are not significant at the 95 % confidence level, based on the Monte Carlo significance test procedure described by Anderson (2007), indicating that there is little difference in the relationship between the CP/EP El Niño and the NPO. Note that the NPO is generally defined as the second leading empirical orthogonal function (EOF2) of the NDJFM North Pacific SLP anomalies poleward of 15°N (e.g., Linkin and Nigam 2008). The correlation between the NDJFM NPO index defined above using the difference between the two poles and that derived from EOF analysis (i.e., the second principal component (PC2) associated with the EOF2) reaches 0.73 (significant at the 99.9 % confidence level). Using the PC2 of the North Pacific SLP anomalies to compute its correlations with the four NINO indices a year later (not shown) is similar to (but less than) using the difference between the two poles.

In addition to the preceding signal over the North Pacific, there is a north–south dipole pattern of negative SLP anomalies over northeastern North America and positive SLP anomalies over the western tropical North Atlantic that also precede the Niño3, Niño3.4, and Niño4 indices by one year. This dipole pattern is most pronounced for the SST indices located closer to the central Pacific (Niño3.4 and Niño4), but becomes weaker for the SST indices located towards the eastern Pacific (Niño3 and Niño1+2), suggesting that the dipole pattern may be more closely linked to the CP El Niño than to the EP El Niño. As will be shown later, the northern and southern poles of this dipole pattern almost correspond with the two action centers of the PNA over North America. For brevity, we hereafter refer to this dipole pattern over northeastern North America to the western tropical North Atlantic as the North American dipole (NAD). To quantitatively depict the NAD signal that precedes ENSO, a simple NAD index was defined as the difference between the normalized (subtracting the mean and then dividing by the standard deviation) SLP anomalies averaged over the southern (93–58°W, 9–29°N) and northern (77–43°W, 53–68°N) poles (indicated by the green boxes in Fig. 1d) of the NAD. Note that the definition of the NAD index (southern pole minus northern pole) is opposite to that of the NPO (northern pole minus southern pole) so that the positive NAD index is associated with the CP El Niño. Given the linear nature of the statistics, it is reasonable to assume that the NAD index of opposite sign would be associated with the CP La Niña.

We note that both the southern poles of the NPO and NAD are located at latitudes between 8°N and 26°N (Fig. 1d). To further test the difference between the SST patterns in the tropical Pacific related to the preceding NPO and NAD, we show in Fig. 2 the cross-correlations between the NDJFM-averaged SLP anomalies meridionally averaged over 8–26°N from the North Pacific across North America to the western North Atlantic, and SST anomalies along the equatorial Pacific (meridionally averaged over 5°S–5°N) a year later. The SST patterns related to the southern poles of the preceding NPO and NAD are nearly reversed in sign in the equatorial Pacific. The significant positive SST anomalies related to the southern pole of the preceding NAD (corresponding to the 100–50°W zone) is located in the central equatorial Pacific (between 160°E and 140°W), with maximum warming near the dateline. In contrast, the significant negative SST anomalies related to the southern pole of the preceding NPO (corresponding

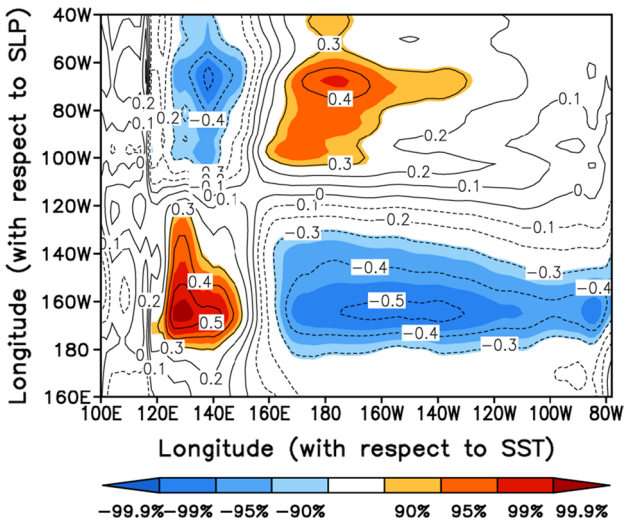

Fig. 2 Cross-correlations between the NDJFM-averaged SLP anomalies meridionally averaged over 8–26°N from the North Pacific across North America to the western North Atlantic (*y-axis*), and SST anomalies along the equatorial Pacific (meridionally averaged over 5°S–5°N) a year later (*x-axis*). Areas with a correlation significant at or above the 90 % confidence level are *shaded*

to the 180–135°W zone) extend much father towards the eastern equatorial Pacific than the positive SST anomalies related to the southern pole of the preceding NAD, with maximum cooling mostly to the east of the dateline. This finding further demonstrates that the NAD, unlike the NPO, appears to be more closely related to the CP El Niño than to the EP El Niño.

In addition, by inspecting the spatial patterns of the winter (NDJFM) averaged SLP anomalies regressed onto the simultaneous NAD and PNA indices (Fig. 3a, b, respectively), we note that the SLP pattern associated with the NAD closely resembles that associated with the PNA, with the below-average SLPs located southwest of Hawaii and over northeastern North America, and above-average SLPs located southeast of the Aleutian Islands and over the southeastern United States and Gulf of Mexico. In the North Atlantic, both the NAD and PNA are associated with a positive phase of the NAO (Barnston and Livezey 1987; Hurrell 1995). The northern and southern poles of the NAD are almost matched to the two action centers of the PNA over North America. The correlation coefficient between the NDJFM-averaged NAD and PNA indices is 0.53 (significant at the 99 % confidence level), which is indicative of a close linkage between the NAD and PNA. This linkage can also be observed in the patterns of SST anomalies regressed onto their respective indices (Fig. 3c, d). The simultaneous SST pattern associated with the NAD is similar to that associated with the PNA, both of which are characterized by a typical EP La Niña pattern in the tropical Pacific, indicating that both the NAD and PNA are closely linked to ENSO. As noted previously (Zhang et al. 1996; Trenberth et al. 1998), ENSO can play an important role in developing the PNA (and hence NAD) via the poleward propagation of Rossby wave trains. Therefore, the NAD develops almost simultaneously with, and is closely related to, tropical ENSO events.

However, we also argue that although the NAD is closely connected to the EP-type ENSO variability, the NAD has its own internal variability independent of ENSO. The partial regression of the NDJFM-averaged SLP anomalies onto the NAD index (with the ENSO signal linearly removed) indicates that the SLP anomalies associated with the NAD are remarkably reduced in most regions of the North Pacific, while they are only slightly reduced in some regions of the North America compared with those obtained without the removal of the ENSO effect (see Fig. 3e, f). Therefore, a distinct NAD-related SLP pattern remains after the ENSO signal is removed. This suggests that in addition to ENSO, the NAD also appears to have its origin in internal dynamics, consistent with the findings of Simmons et al. (1983) who found that the internal atmospheric dynamical processes in the midlatitude could generate a PNA-like pattern through the barotropic and baroclinic instability.

3.2 Establishing the NAD–CP El Niño relationship

The time series of the winter (NDJFM) averaged NAD index and four NINO indices during the following winter are plotted in Fig. 4a and their correlation coefficients are listed in Table 1. The correlations strengthen for the NINO indices located towards the central Pacific. In particular, the Niño4 index has a correlation coefficient of 0.44 (significant at the 95 % confidence level) with the preceding NAD index, which is higher than that between the Niño3 index with the preceding NAD index ($R = 0.27$, not significant at the 95 % confidence level). The difference between these two correlations is significant at the 95 % confidence level, based on the Monte Carlo significance test procedure (Anderson 2007). The Niño1+2 index exhibits a very weak correlation ($R = 0.15$) with the preceding NAD index.

Ren and Jin (2011) developed two new indices that separately identify the two types of El Niño events through a simple transformation of the Niño3 and Niño4 indices. They argued that unlike the Niño3 and Niño4 indices, the two new indices have a little simultaneous correlation. We also computed the correlations of the winter NAD index with the following winter CP and EP El Niño indices developed by Ren and Jin (2011). The correlations are 0.41 for CP El Niño and 0.24 for EP El Niño. The difference between these two correlations is also significant at the 95 % confidence level. These results support the idea that the NAD appears to be more closely linked to the CP El Niño than to the EP El Niño.

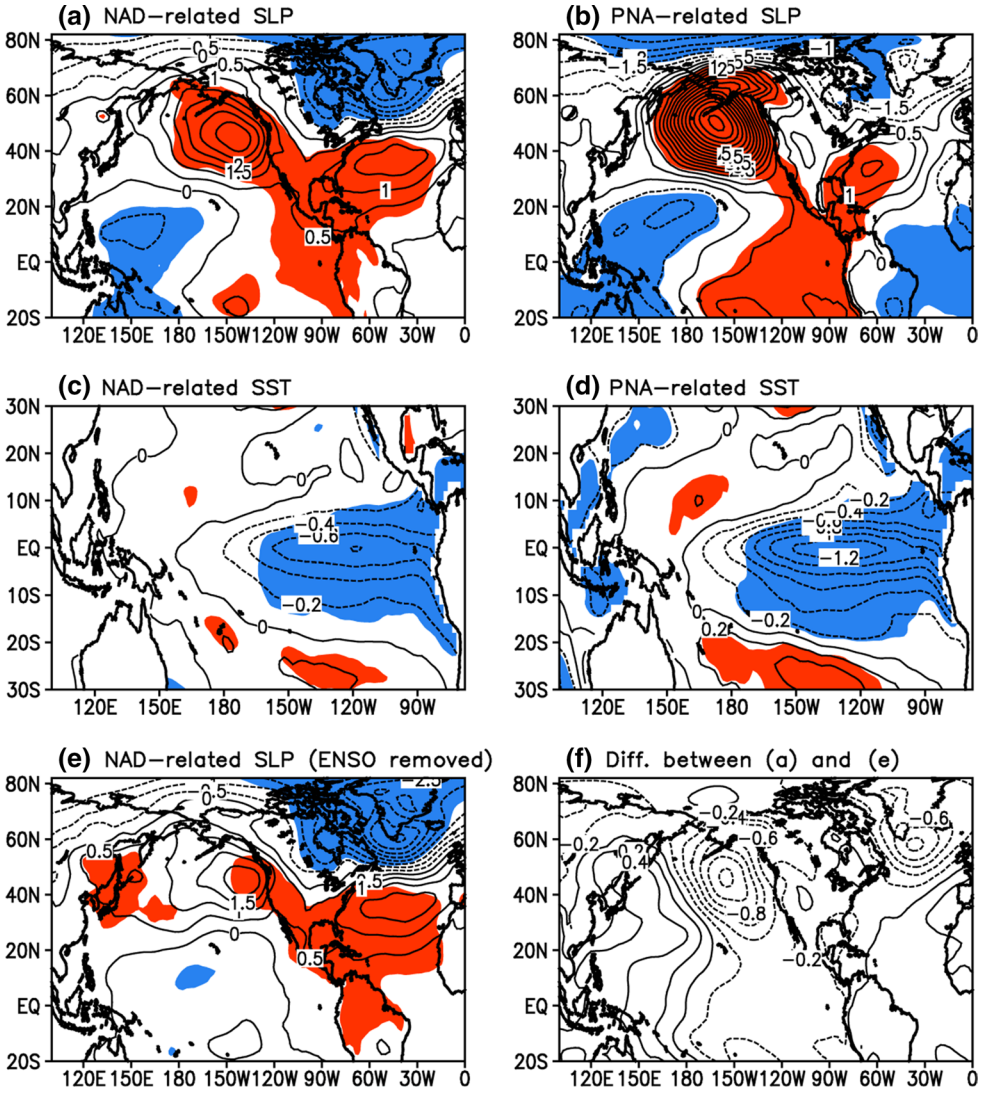

Fig. 3 **a** Regression of the winter (NDJFM) averaged SLP anomalies (contour interval 0.5 mbar) on the simultaneous NAD index. **b** As in **a** but for regression of the winter averaged SLP anomalies on the PNA index. **c** Regression of the winter averaged SST anomalies (contour interval 0.2 °C) on the simultaneous NAD index. **d** As in **c** but for regression of the winter averaged SST anomalies on the PNA index. **e** Regression of the winter averaged SLP anomalies (contour interval 0.5 mbar) on the simultaneous residual NAD index, obtained by linearly removing the winter Niño3.4 SST from the original NAD index. **f** Difference between **a** and **e** (contour interval 0.2 mbar). In **b** and **d**, the sign of the PNA index is reversed for comparison. In **a**–**e**, positive (*red*) and negative (*blue*) SLP or SST anomalies, significant at the 95 % confidence level, are *shaded*

Figure 4b shows the regression of winter (NDJFM) averaged SST anomalies in the tropical Pacific onto the previous winter NAD index. Significant positive SST anomalies associated with the preceding NAD are concentrated in the central tropical Pacific between 160°E and 120°W, covering the Niño3.4 and Niño4 regions. In addition, there are significant negative SST anomalies in the western tropical Pacific and weak positive, or even negative, SST anomalies in the eastern tropical Pacific that are also related to the preceding NAD. This preceding NAD-related SST anomaly pattern closely resembles a typical CP El Niño pattern (Larkin and Harrison 2005; Ashok et al. 2007; Kao and Yu 2009; Kug et al. 2009).

Previous work has shown that the events of 1990/1991, 1994/1995, 2002/2003, 2004/2005, and 2009/2010 were typical CP El Niño events (Kug et al. 2009; Yu and Kim 2010). We constructed composites of the previous winter (NDJFM) averaged SLP anomalies for these CP El Niño events (Fig. 5a), and for comparison constructed composites of the previous winter averaged SLP anomalies for two typical EP El Niño events (1982/1983 and 1997/1998; Fig. 5b). Composite SLP anomalies preceding CP El Niño events exhibit significant positive SLP anomalies over the North Pacific poleward of 20°N as well as an NAD-like pattern over eastern North America to the western tropical North Atlantic. In contrast, composite SLP anomalies preceding EP El Niño events only exhibit a marked NPO-like pattern over the North Pacific; the NAD-like pattern over eastern North America to the western tropical North Atlantic becomes indistinct.

The above results indicate a close connection between the winter NAD and CP El Niño events during the following winter. To further elucidate the lagged relationship between the NAD and CP El Niño, we performed a maximum covariance analysis (MCA; also known as singular value decomposition (SVD); Bretherton et al. 1992)

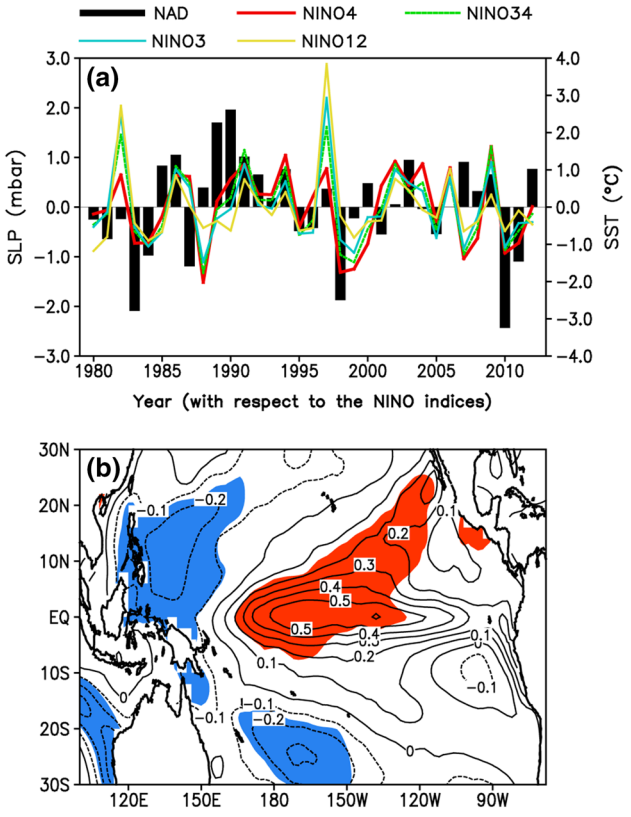

Fig. 4 **a** Time series of the winter (NDJFM) averaged NAD index (*black bars*), Niño1+2 (*yellow line*), Niño3 (*light blue line*), Niño3.4 (*dashed green line*), and Niño4 (*red line*) indices a year later. All indices are standardized, and the correlation coefficients of the NAD index with four NINO indices a year later are given in Table 1. **b** Regression of the winter averaged SST anomalies (contour interval 0.1 °C) in the tropical Pacific onto the previous winter NAD index. Positive (*red*) and negative (*blue*) SST anomalies, significant at the 95 % confidence level, are *shaded*

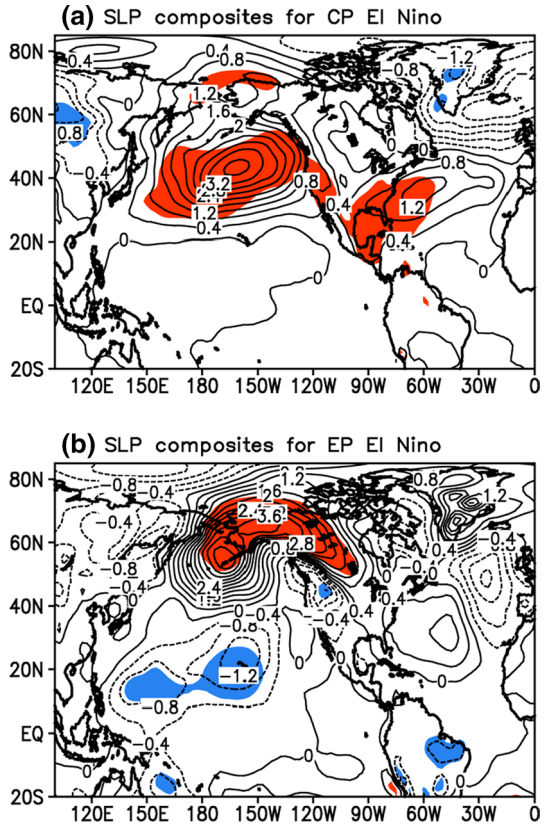

Fig. 5 **a** Composites of the previous winter (NDJFM) averaged SLP anomalies (contour interval 0.4 mbar) for five strong CP El Niño events (1990–1991, 1994–1995, 2002–2003, 2004–2005, and 2009–2010). **b** Composites of the previous winter averaged SLP anomalies for two strong EP El Niño events (1982–1983 and 1997–1998). In **a** and **b**, positive (*red*) and negative (*blue*) SLP anomalies, significant at the 95 % confidence level, are *shaded*

of the cross-covariance matrix between the NDJFM-averaged SLP anomalies over North America and the western Atlantic (120–30°W, 0–85°N) and the tropical Pacific (125°E–75°W, 20°S–20°N) SST anomalies a year later. The leading MCA mode explains 72 % of the total squared covariance. The correlation coefficient between the corresponding expansion coefficient time series is 0.49 (significant at the 99 % confidence level; Fig. 6c). These statistical results indicate that the two fields included in the MCA are strongly coupled.

Figure 6a, b show the leading pair of heterogeneous patterns, which were generated by correlating the respective heterogeneous SLP and SST fields with the time series of the leading MCA normalized expansion coefficient. The SLP pattern in Fig. 6a shows a meridional dipole pattern over northeastern North America to the western tropical North Atlantic, with centers of action on either side of about 40°N, which resembles the NAD pattern shown in Fig. 3a. The strong correspondence between the MCA SLP expansion coefficient and the NAD index ($R = 0.92$) indicates that this SLP pattern obtained from the MCA is dominated by the NAD-related pattern. During the following winter, the tropical Pacific SST anomaly pattern in Fig. 6b is dominated by a zonal tripole pattern, which is characterized by positive SST anomalies in the central tropical Pacific and negative SST anomalies in the western and eastern tropical Pacific. We note that this MCA SST pattern strongly resembles the CP El Niño pattern (Larkin and Harrison 2005; Ashok et al. 2007; Kao and Yu 2009; Kug et al. 2009). The time series of the MCA SST expansion coefficient is also closely correlated with that of the Niño4 index ($R = 0.94$). These results are consistent with our conclusions derived from Figs. 4 and 5, and further confirm the existence of a close connection between the NAD and CP El Niño a year later.

Our analysis suggests that the NAD and PNA are related to one another. However, correlation maps of the NDJFM-averaged PNA index with the tropical Pacific

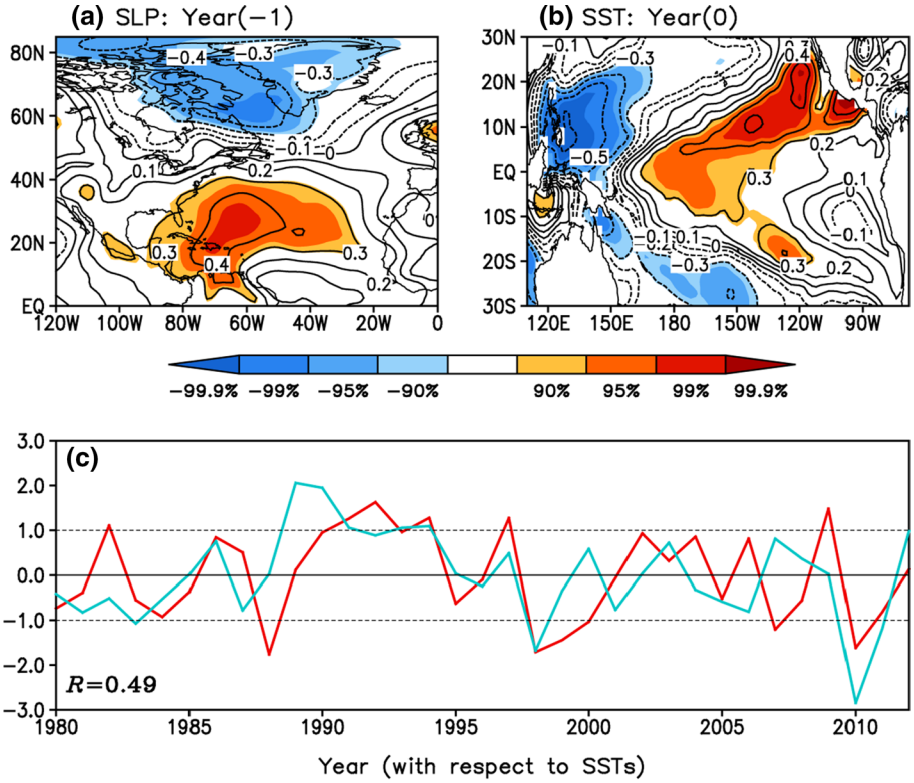

Fig. 6 Spatial properties of the leading MCA mode for **a** the winter (NDJFM) averaged SLP anomalies in North America and the western Atlantic (120–30°W, 0–85°N) and **b** the tropical Pacific (125°E–75°W, 20°S–20°N) SST anomalies a year later, shown as correlation maps of the respective heterogeneous SLP and SST fields with the MCA leading normalized expansion coefficients. **c** The MCA leading normalized expansion coefficients of the winter SLP field (*light blue line*) and the tropical Pacific SST field a year later (*red line*). In **a** and **b**, areas with correlations significant at or above the 90 % confidence level are *shaded*. In **c**, the correlation between the two time series is given in the *lower left corner*, and the *horizontal dashed lines* indicate ±1 standard deviation

SST anomalies a year later indicate that the preceding PNA-related warming extends farther east than the preceding NAD-related warming, and the eastern equatorial Pacific SST related to the preceding PNA is dominated by significant positive (not negative) anomalies (Fig. 7a). Furthermore, the preceding PNA-related maximum warming is located in the equatorial Pacific between 170°W and 125°W, covering almost the entire Niño3.4 region (170–120°W, 5°S–5°N), rather than the Niño4 region (160°E–150°W, 5°S–5°N) where the preceding NAD-related warming center is located (Fig. 4b). It seems that the PNA is followed not simply by a typical CP El Niño pattern, but by a mixed CP and EP El Niño pattern. A possible explanation for this difference may be that the PNA has its own related SLP anomalies independent of the NAD (Fig. 7b). As shown later, it is exactly SLP anomalies associated with the NAD over northeastern North America to the western tropical North Atlantic that play an important role in developing the CP El Niño. Note in Fig. 7b that SLP anomalies related to the PNA but independent of the NAD are located mainly in the tropics and North Pacific. It is likely that these SLP anomalies related to the PNA, but independent of the NAD, subsequently cause the positive SST anomalies to extend much farther toward the eastern equatorial Pacific than those associated with the NAD. Therefore, the PNA, like the NPO, tends to be followed by a mixed CP and EP El Niño pattern, rather than a typical CP El Niño.

3.3 Possible mechanisms linking the NAD to CP El Niño

The above results show a statistically significant lead–lag relationship between variability in the NAD and the CP El Niño. But how does the NAD affect CP El Niño? Next, we examine in detail the evolutions of SST, surface wind, precipitation, and subsurface ocean temperature anomalies associated with the NAD, with the aim of identifying how the evolution of these anomalies is related to the development of SST anomalies associated with CP El Niño events. To isolate the impact of the NAD on the tropical Pacific climate variability, the ENSO effect (represented by the DJF-averaged Niño3.4 SST) is first removed from the original DJF-averaged NAD index, yielding the residual NAD index, and then the lagged correlation is obtained based on the residual NAD index.

We first examine the evolutions of SST, surface wind, and precipitation anomalies associated with the NAD. Figure 8 shows the spatial patterns of the DJF-averaged residual NAD index correlated with 3-month averaged SST, surface wind, and precipitation anomalies for DJF concurrent with the NAD index, and several lead times (MAM, JJA, and SON). During winter (the DJF season; Fig. 8a), there is a horseshoe-like SST anomaly pattern in the northeastern Pacific and a tripole-like SST anomaly pattern in the North Atlantic that are associated with the NAD. These extratropical SST anomalies are possibly a

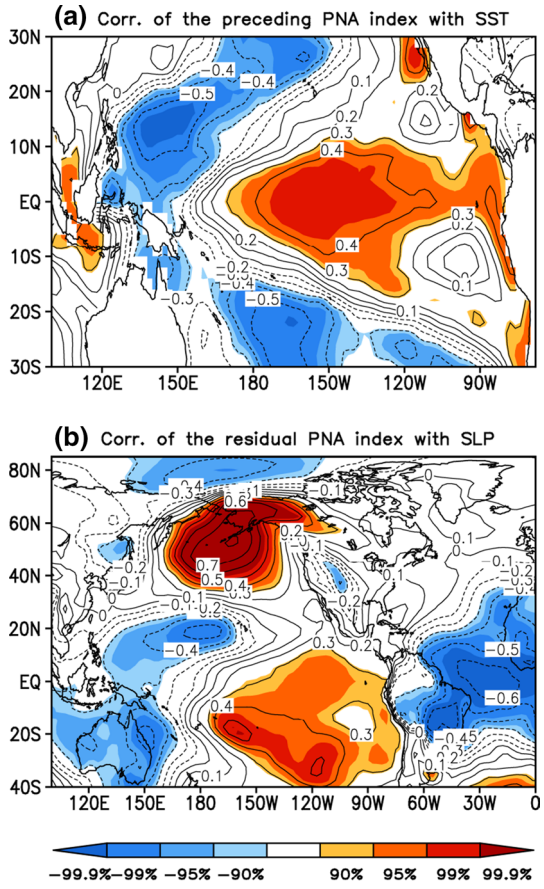

Fig. 7 **a** Correlation map of the winter (NDJFM) averaged SST anomalies in the tropical Pacific with the previous winter PNA index. **b** Correlation map of the winter averaged SLP anomalies with the simultaneous residual PNA index, obtained by linearly removing the winter averaged NAD index from the original winter averaged PNA index. In **a** and **b**, areas with correlations significant at or above the 90 % confidence level are *shaded*

direct oceanic response to the forcing of extratropical SLP anomalies associated with the NAD. The NAD is associated with anomalous SLPs located southeast of the Aleutian Islands in the North Pacific and a positive phase of the NAO in the North Atlantic (Fig. 3a), and surface wind anomalies associated with the NAD are consistent with these SLP anomalies. Anomalous surface winds associated with the NAD can force a tripole-like SST pattern in the North Atlantic via changes in the latent heat flux (not shown), giving rise to significant negative SST anomalies in the northern tropical Atlantic (NTA) region. The NTA SST cooling then induces southwestward wind anomalies via modifying the cross-equatorial pressure gradient, adding to the back-ground northeasterly winds and increasing the wind speed in the NTA region. The increased winds increase the latent heat flux release from the oceans to the atmosphere that reinforces the initial SST cooling, forming a positive wind–evaporation–SST (WES) feedback (Xie and Philander 1994). This WES feedback causes the NTA SST anomalies to develop.

During spring (the MAM season; Fig. 8b), after three months after the NAD peaks, the NTA SST cooling reaches its maximum. The NTA SST warming (cooling) is known to be capable of enhancing (reducing) local convection, especially over the equatorial Atlantic where the Atlantic Intertropical Convergence Zone (ITCZ) is located, and the enhanced (reduced) local convection in turn generates a low-level cyclonic (anticyclonic) flow over the subtropical northeastern Pacific as a Gill-type Rossby-wave response (Ham et al. 2013a). We note that in Fig. 8b, the suppression in convection associated with the NAD-induced NTA cooling is clear over the off-equatorial region in the vicinity of the Atlantic ITCZ, and this suppressed convection over the Atlantic ITCZ associated with the NAD gives rise to a low-level anticyclonic flow over the subtropical northeastern Pacific, consistent with the findings of Ham et al. (2013a). The anticyclonic flow then produces a southerly flow on its west flank, which leads to surface warming through the weakened northeasterly trade winds and low-level convergence, resulting in enhanced precipitation over the subtropical northeastern Pacific.

During summer (the JJA season; Fig. 8c), the positive precipitation anomalies associated with the NAD are mostly concentrated over the central-eastern subtropical Pacific ITCZ region owing to the northward migration of the ITCZ. The associated diabatic heating can give rise to a low-level cyclonic flow anomaly over the western North Pacific (Ham et al. 2013a). This cyclonic flow enhances the southerly flow at its eastern edge, which may act to further strengthen positive SST and precipitation anomalies over the subtropical Pacific. This thermodynamic coupling among positive precipitation, the southerly flow, and positive SST anomalies leads to a westward and equatorward extension of positive precipitation and SST anomalies. As the cyclonic flow over the western North Pacific is gradually strengthened through air–sea feedback, it induces anomalous westerlies in the western equatorial Pacific, combined with anomalous easterlies in the eastern equatorial Pacific induced by the anticyclonic flow over the subtropical northeastern Pacific, which lead to convergence in the central equatorial Pacific, and in turn trigger the warming there. Because anomalous easterlies persist in the eastern equatorial Pacific, they can subsequently suppress SST warming in the eastern Pacific by anomalous upwelling through Ekman transport and by excessive evaporation driven by enhanced trade winds (Kug et al. 2009). Therefore, the SST warming develops mainly in the central Pacific, and cannot extend to the eastern Pacific. This warming is trapped and sustained in the central equatorial Pacific by local air–sea coupling processes (Kao and Yu 2009). Finally, a CP El Niño pattern is

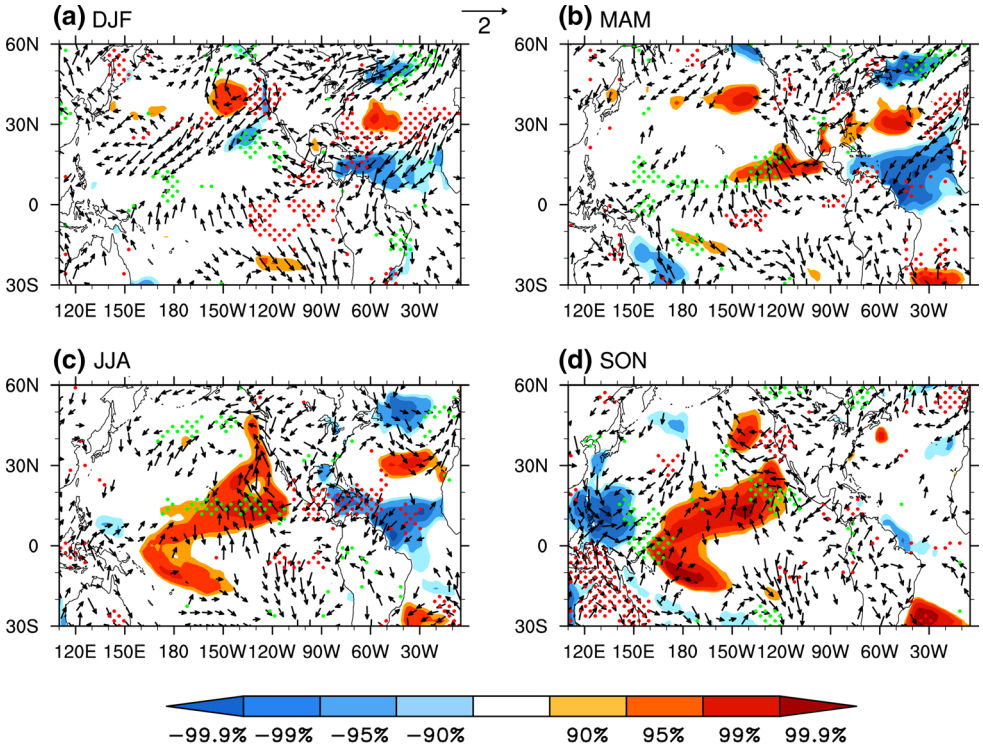

Fig. 8 Correlation maps of the DJF-averaged NAD index with the 3-month averaged SST (*shading*), surface wind (*vectors*), and precipitation (*stippled*) anomalies for **a** DJF concurrent with the NAD index, and several lead times (**b** MAM, **c** JJA, and **d** SON) for the period 1979–2013. Positive (*red*) and negative (*blue*) SST anomalies with correlations significant at or above the 90 % confidence level are *shaded*. Positive (*green*) and negative (*red*) precipitation anomalies with correlations significant at the 90 % confidence level are *stippled*. Only surface wind vectors significant at the 90 % confidence level are shown

established in the tropical Pacific during the SON season (Fig. 8d).

The above analyses suggest that the NTA SST anomalies induced by the NAD play an important role in developing subsequent CP El Niño events. The results provide further observational evidence of the influence of the NTA SST on the CP El Niño, as described by Ham et al. (2013a). In general, the underlying physical process associated with the effects of the NAD-induced NTA SST on CP El Niño is similar to the mechanism proposed by Ham et al. (2013a) to explain the influence of the NTA SST on subsequent CP El Niño events. Despite the overall similarity between the mechanisms described here and by Ham et al. (2013a), however, the emphasis here is on the connection between the NAD and CP El Niño, rather than on the NTA SST and CP El Niño. Our analysis indicates that the NAD may serve as an important source of atmospheric forcing to excite the NTA SST, while the latter may play a particularly important role in transmitting the atmospheric forcing of the NAD into the tropical Pacific to impact the CP El Niño state. That is, a systematic cause-and-effect relationship among the NAD, NTA SST, and CP El Niño may exist as follows: NAD (winter) → NTA SST (spring) → CP El Niño (winter of the next year), which was not addressed previously. This NAD → NTA SST → CP El Niño dynamic link highlights the potential importance of the NAD in contributing the development of the CP El Niño. Further research is necessary to investigate the physical processes associated with the NAD → NTA SST → CP El Niño dynamic link, as well as its role in affecting the prediction of the CP El Niño.

The process described above involves surface air–sea coupling associated with the NAD in the NTA and tropical Pacific. Kao and Yu (2009) reported that the development of CP El Niño events appears to be less related to thermocline variations and may involve only local ocean–atmosphere interaction; this differs from the EP El Niño, which is associated with basin-wide thermocline variations. We then examine the evolutions of subsurface ocean temperature anomalies associated with the NAD. Figure 9 shows correlation maps of the DJF-averaged residual NAD index with the 3-month averaged subsurface temperature anomalies at different depths averaged over 5°S–5°N for DJF concurrent with the NAD index, and several lead times (MAM, JJA, and SON). During winter (the DJF season; Fig. 9a), there are significant positive subsurface temperature anomalies in the central equatorial Pacific at around 50–250 m depth. These positive subsurface temperature anomalies are likely generated by the NAD-related surface wind anomalies. Note in Fig. 8a that the anticyclonic flow associated with the NAD extends westward from the NTA into the subtropical northeastern Pacific during winter. The anticyclonic flow over the subtropical northeastern Pacific gives rise to an equatorial easterly flow on its south flank, which induces low-level convergence in the central equatorial Pacific. In turn, the convergence leads to positive subsurface temperature anomalies in the central equatorial Pacific. After DJF, these positive subsurface temperature anomalies

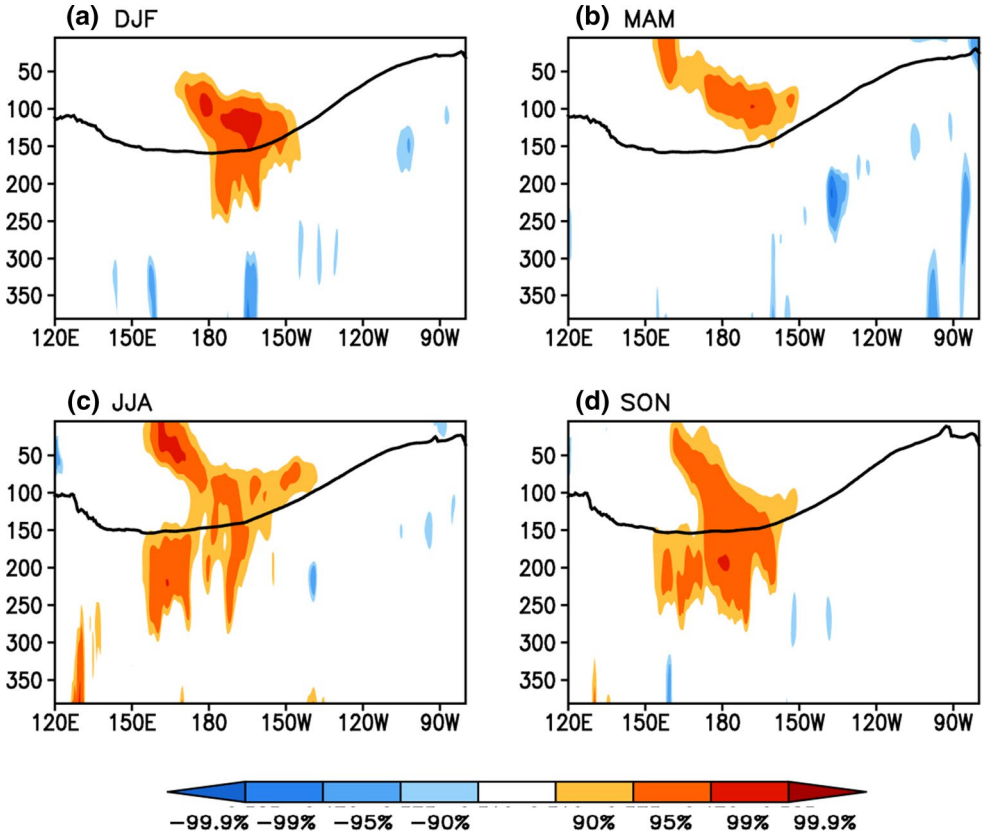

Fig. 9 Correlation maps of the DJF-averaged NAD index with the 3-month averaged subsurface temperature anomalies at different depths averaged over 5°S–5°N for **a** DJF concurrent with the NAD index, and several lead times (**b** MAM, **c** JJA, and **d** SON) for the period 1979–2010. Areas with correlation significant at or above the 90 % confidence level are shaded. *Thick black contour* indicates the climatological position of the 23 °C isotherm

associated with the NAD do not show an apparent eastward and upward propagation along the subsurface pycnoclines, possibly due to the local easterlies in the eastern equatorial Pacific as a part of the anticyclonic flow (Ham et al. 2013a). Therefore, the subsurface temperature anomalies cannot extend to the eastern Pacific, but instead exhibit weak and near-local fluctuations. These subsurface temperature anomalies are sustained in the central equatorial Pacific (between 150°E and 150°W) by local ocean–atmosphere interaction (Kao and Yu 2009), and do not reach the near-surface layer in the eastern equatorial Pacific until SON. This finding is generally consistent with the view that the development of the CP El Niño is characterized by local (not basin-wide) subsurface temperature variations in the central equatorial Pacific (Kao and Yu 2009; Kug et al. 2009).

Our results have shown that the NAD can induce both the westerlies in the western equatorial Pacific and easterlies in the eastern equatorial Pacific at the same time. We argue that because of this opposite low-level wind anomalies between the western and eastern equatorial Pacific, the surface warming mainly develops in the central Pacific, rather than in the eastern Pacific. Thus, we conclude that, unlike the NPO or PNA, the NAD tends to be closely linked to the CP El Niño, implying that the NAD may play a unique role in developing the CP El Niño different from the influences of the NPO or PNA.

3.4 Important role of the NAD in forcing the NTA SST anomalies

The results presented above indicate that the NAD can influence the NTA SST, and the NTA SST may subsequently play an important role in developing subsequent CP El Niño events. We now turn to the relationship between the NAD and NTA SST, with the aim of further emphasizing the importance of the NAD in forcing the NTA SST anomalies. First of all, we compute lead–lag correlations between the DJF-averaged NAD index and 3-month area-averaged NTA SST over (85°W–20°E, 0–15°N) (Fig. 10). The peak correlation ($R = -0.76$; significant at the 99.9 % confidence level) occur during FMA, lagging the peak of the NAD during DJF by about 2 months, indicating a lag response of the NTA SST to the NAD atmospheric forcing. This suggests that the DJF NAD may account for a large fraction (~60 %) of the NTA SST variability during the FMA season. Then, we calculate the partial regression of the FMA-averaged NTA SST onto the tropical Pacific SST anomalies in the following winter (DJF) by linearly removing the NAD index from the previous winter (Fig. 11b). With the removal of the NAD effect, regressions in most regions of the tropical Pacific are substantially reduced compared with those obtained without the removal of the NAD effect (Fig. 11a). These results support the idea that

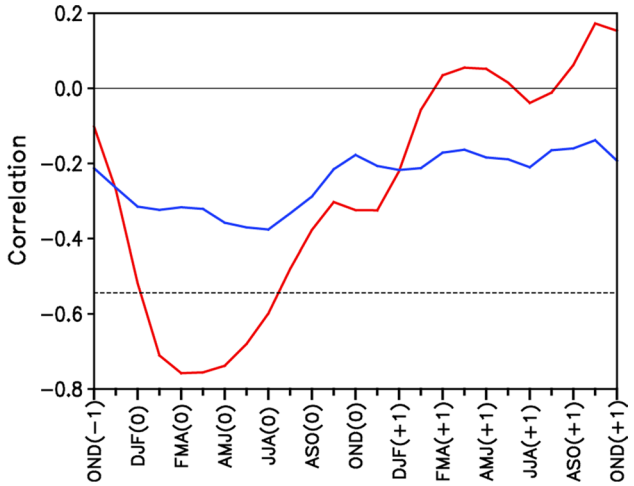

Fig. 10 Lead–lag correlations of the DJF-averaged NAD and NAO indices with the overlapping 3-month averaged values of the NTA SST over (85°W–20°E, 0–15°N) (–1: year prior to the NAD index; 0: year concurrent with the NAD index; +1: year followed by the NAD index). *The horizontal dashed line* shows the 99.9 % significance level

the NAD can provide a major source of atmospheric forcing to excite the NTA SST, and the latter subsequently serves an ocean bridge linking the NAD to the CP El Niño.

In addition to the influence of ENSO through the PNA/NAD pattern, the NTA SST is affected in part by the NAO variability. Atmospheric anomalies associated with the NAO can produce a tripole-like SST pattern in the North Atlantic that has previously been noted in the literature (Cayan 1992; Deser and Timlin 1997; Marshall et al. 2001; Pan 2005). This leads us to question the influence of the NAO on the CP El Niño. However, we found that although the wintertime NAO forcing can lead to anomalous SSTs in the NTA, the NAO is not followed by a distinct CP El Niño pattern (Fig. 11c). Furthermore, with the removal of the NAO effect, regressions of the FMA-averaged NTA SST onto the tropical Pacific SST anomalies in the following winter (DJF) (Fig. 11d) do not change substantially compared with those obtained without the removal of the NAO effect (Fig. 11a). These results suggest that the influence of the NAO on the subsequent CP El Niño is generally weaker than is that of the NAD.

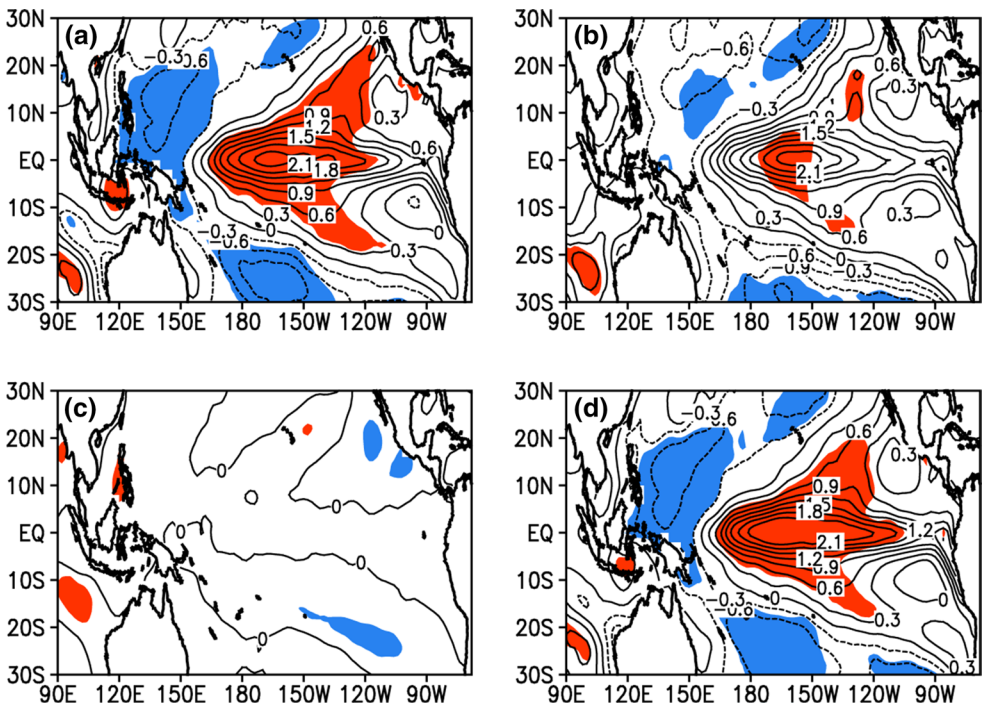

Fig. 11 **a** Regression of the winter (DJF) averaged SST anomalies (contour interval 0.3 °C) in the tropical Pacific onto the NTA SST over (85°W–20°E, 0–15°N) during the previous FMA season. **b** Partial regression of the FMA-averaged NTA SST onto the tropical Pacific SST anomalies in the following winter by linearly removing the NAD index from the previous winter. **c** Regression of the winter averaged SST anomalies in the tropical Pacific onto the previous winter NAO index. **d** Partial regression of the FMA-averaged NTA SST onto the tropical Pacific SST anomalies in the following winter by linearly removing the NAO index from the previous winter. In **a**, **b**, and **d**, the sign of the NTA SST is reversed for comparison. In **a**–**d**, positive (*red*) and negative (*blue*) SST anomalies, significant at the 95 % confidence level, are *shaded*

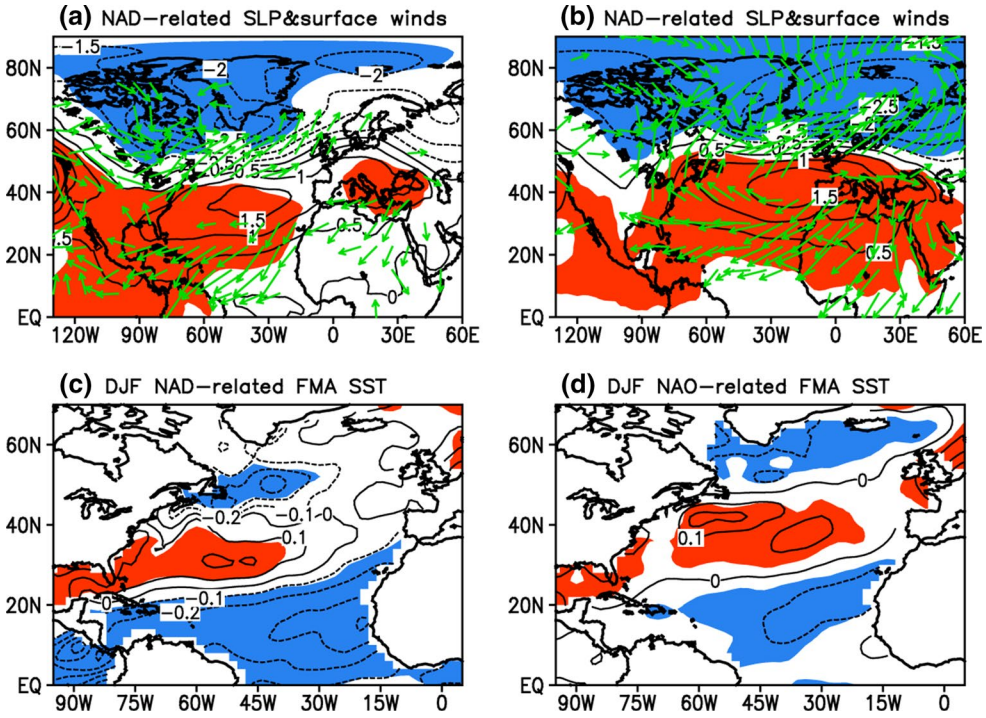

Fig. 12 **a** Regression of the DJF SLP (mb; contours) and surface wind (m s^{-1}; vectors) anomalies on the simultaneous NAD index. **b** As in **a** but for regression of the DJF SLP anomalies on the NAO index. **c** Regression of the FMA SST anomalies (°C; contours) on the NAD index of the previous DJF season. **d** As in **c** but for regression of the FMA SST anomalies on the NAO index of the previous DJF season. In **a** and **b**, only surface wind vectors significant at the 95 % level are shown. In **a**–**d**, positive (*red*) and negative (*blue*) SLP or SST anomalies, significant at the 95 % confidence level, are *shaded*

It is important to point out that the NAD and NAO are interconnected because their related SLP anomalies overlap over some regions of the North America and western North Atlantic. The DJF NAD and NAO indices have a correlation of 0.52 (significant at 99 % confidence level) for the period 1979–2013. Given that both the NAO and NAD exert influence on the NTA SST, the question naturally arises as to why the NAD can excite the CP El Niño while the NAO cannot. One possible reason is that the NTA SST is more influenced by the NAD than the NAO. Figure 12a, b show the DJF SLP and surface wind anomalies regressed onto the simultaneous NAD and NAO indices, respectively. We note that the centers of action of the NAD and NAO in the North Atlantic are not coincident: NAD-related SLP anomalies are shifted southward and westward respectively by about 5° and 30° with respect to the centers of action of the NAO. Consistent with SLP anomalies, significant surface wind anomalies associated with the NAD extend much farther west and south towards the NTA region than those associated with the NAO. Accordingly, despite the fact that both the NAD and NAO during the DJF season are closely linked to a tripole-like SST pattern in the North Atlantic of the following FMA season, their resulting tripole-like SST patterns are substantially different in the North Atlantic, especially in the NTA region where the NTA SST anomalies induced by the NAO have smaller amplitudes than those induced by the NAD (Fig. 12c, d). The correlation ($R = -0.32$) between the DJF NAO index and the following FMA NTA SST is much lower than that ($R = -0.76$) between the DJF NAD index and the following FMA NTA SST (Fig. 10). These results suggest that the NAD, rather than the NAO, is most effective at forcing the NTA SST anomalies. Therefore, in contrast to the NAO, the NAD may play a vital role in influencing the occurrence of the CP El Niño, owing to its effectiveness at forcing the NTA SST anomalies.

3.5 Joint role of the NAD and NPO in initiating the onset of CP El Niño events

As mentioned in the Introduction, previous studies have identified the NPO as a precursor signal for CP/EP El Niño events (Vimont et al. 2001, 2003a,b; Anderson 2003; Alexander et al. 2010; Yu and Kim 2011). Considering that both the NAD and NPO influence subsequent CP El Niño events, it is of interest to explore their joint relationship with the onset of CP El Niño events.

Scatterplots of the winter (NDJFM) averaged NAD index versus the Niño4 index during the following winter, plotted only for those years in which the NAD index has the same and opposite signs as the NPO index, are shown in Fig. 13a, b, respectively. The preceding NAD index is much more strongly correlated with the Niño4 index if the NAD index has the same sign as the NPO index ($R = 0.53$; significant at the 95 % confidence level for the 20 events) compared with years in which they have the opposite sign ($R = 0.08$; not significant even at the 90 % confidence level for the 13 events). The difference in these two correlations is statistically significant at the 95 % confidence level, based on the Monte Carlo

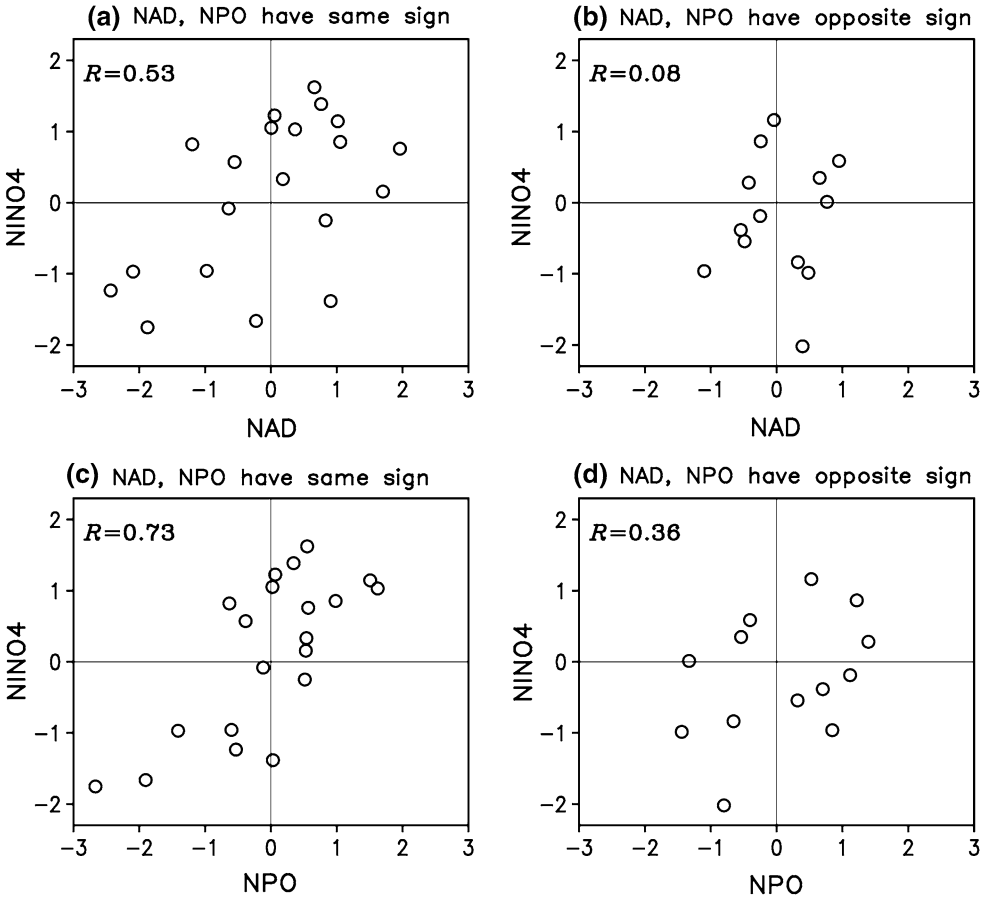

Fig. 13 **a** Scatterplot of the winter (NDJFM) averaged NAD index versus the Niño4 index a year later, plotted only for those years in which the NAD index has the same sign as the NPO index. **b** As for **a** but for only those years in which the NAD index has the opposite sign as the NPO index. **c** Scatterplot of the winter (NDJFM) averaged NPO index versus the Niño4 index a year later, plotted only for those years in which the NAD index has the same sign as the NPO index. **d** As for **c** but for only those years in which the NAD index has the opposite sign as the NPO index. The correlation coefficient between the winter NAD or NPO index with the Niño4 index a year later is given in the *upper left corner*

Table 2 Classification of CP El Niño years in which the preceding NAD and NPO indices have the same or opposite sign

	NAD, NPO have same sign	NAD, NPO have opposite sign
CP El Niño years	1990/1991, 1994/1995, 2002/2003, 2009/2010	2004/2005

significance test procedure (Anderson 2007). The correlation of the NPO index with the Niño4 index a year later is also higher if the NAD index is accompanied by the NPO index of the same sign ($R = 0.73$; significant at the 99.9 % confidence level for the 20 events) compared with years in which the NPO index is of the opposite sign ($R = 0.36$; not significant even at the 90 % confidence level for the 13 events); the difference between both correlations is also statistically significant at the 95 % confidence level. Furthermore, we found that from 1979 to 2013, there are four CP El Niño events (1990/1991, 1994/1995, 2002/2003, and 2009/2010) that are preceded by same-sign NAD and NPO indices, while there is only one CP El Niño event (2004/2005) that is preceded by opposite-sign NAD and NPO indices (Table 2). These results suggest that the CP El Niño events following the NAD/NPO anomalies are more likely to happen when the NAD and NPO indices are of the same sign.

To provide one possible physical interpretation for these statistical findings presented above, we classified all of the NAD events according to their link with the NPO into the following two groups: (1) positive (negative) NAD events that occur simultaneously with a positive (negative) NPO event (hereafter positive NAD/NPO or negative NAD/NPO), and (2) positive (negative) NAD events that occur simultaneously with a negative (positive) NPO event (hereafter positive NAD/negative NPO or negative NAD/positive NPO; Table 3). A positive or negative NAD event is defined as a year when the NDJFM-averaged NAD index is greater than 0.5 positive standard deviations or less than 0.5 negative standard deviations. The definition of a NPO event is the same as that of an NAD event.

Figure 14 shows the composite differences in the 3-month averaged SST and surface wind anomalies between positive NAD/NPO and negative NAD/NPO (left panel), and between positive NAD/negative NPO and

Table 3 Classification of years in which positive or negative NAD events occur simultaneously with a positive or negative NPO event during the period 1979–2013

	Positive NPO	Negative NPO
Positive NAD	1985, 1986, 1989, 1990, 1991, 2009	2005, 2011
Negative NAD	1992, 2012	1983, 1984, 1987, 1998, 2010

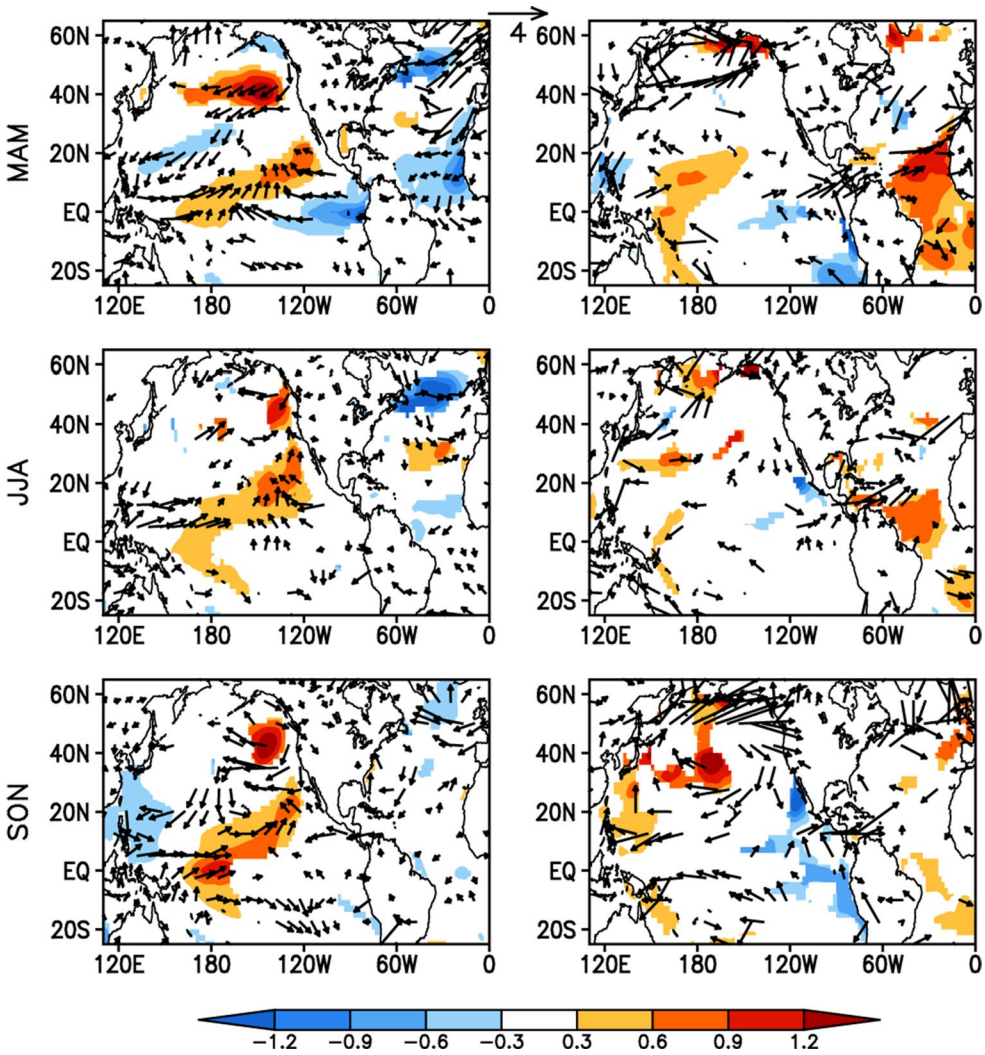

Fig. 14 Composite differences of the 3-month averaged SST (°C; *shading*) and surface wind (m s^{-1}; *vectors*) anomalies between positive NAD/NPO and negative NAD/NPO (*left panel*), and between positive NAD/negative NPO and negative NAD/positive NPO (*right panel*) for (*top to bottom*) MAM, JJA, and SON. Only SST anomalies and surface wind vectors significant at the 95 % confidence level are shown

negative NAD/positive NPO (right panel) for MAM, JJA, and SON. Note that in Fig. 14, the Niño3.4 SST from the previous winter (DJF) is linearly removed from the 3-month averaged SST and surface wind anomalies. For the same-sign NAD/NPO composites, there is a marked horseshoe-like SST pattern in the northeastern Pacific and a marked tripole-like SST pattern in the North Atlantic during MAM. The southern pole of the NPO tends to strengthen the anticyclonic flow over the subtropical northeastern Pacific and the cyclonic flow over the western North Pacific that are induced by the NTA SST. As a result, westerly anomalies over the western equatorial Pacific and easterly anomalies over the eastern equatorial Pacific strengthen during JJA, which can produce a subsequent increase in convergence in the central equatorial Pacific, finally leading to significant warming in the central equatorial Pacific. Conversely, for the opposite-sign NAD/NPO composites, the anticyclonic flow over the subtropical northeastern Pacific and the cyclonic flow over the western North Pacific become indistinct. The convergence of surface winds in the central equatorial Pacific does not start until JJA, thereby limiting the initiation of CP El Niño events.

Overall, the results presented above indicate that the NAD influence on the tropical Pacific interfere or interact with the NPO effect, and the ability of the NAD anomalies in a particular winter to initiate CP El Niño events in

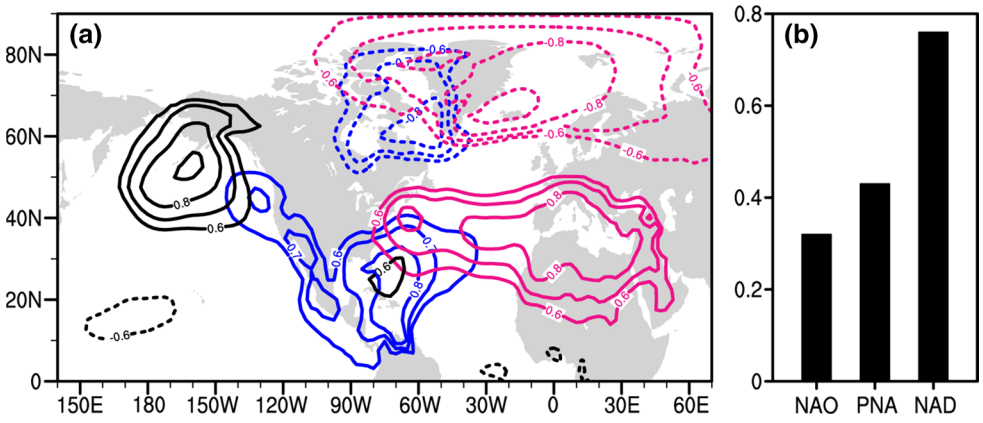

Fig. 15 **a** Correlation maps of the winter (NDJFM) averaged SLP anomalies with the simultaneous PNA (*black contours*), NAD (*blue contours*), and NAO (*red contours*) indices. The contour interval is 0.1. Only correlations greater than 0.6 are shown. **b** Correlations of the DJF-averaged PNA, NAD, and NAO indices with the following FMA NTA SST. For the NAD and NAD, the sign of correlations is reversed for comparison

the following winter is dependent upon the existence of the simultaneous NPO signature in the North Pacific, and vice versa. Furthermore, we note that there is a very weak correlation (<0.05) between the winter (NDJFM) averaged NAD and NPO indices for the period 1979–2013, suggesting that the NAD is relatively independent of the NPO. Given the independence of the NAD and NPO and their joint relationship with the CP El Niño, it is important to consider the status of the NPO when judging whether an NAD event is followed by a CP El Niño event or not. If the wintertime NAD is of the same sign as the NPO, there would be a much higher probability (compared with the opposite-sign NAD/NPO situation) that the NAD is followed by CP El Niño events.

4 Summary and discussion

This study has established a north–south dipole pattern of SLP anomalies showing negative anomalies over northeastern North America and positive anomalies over the western tropical North Atlantic that precedes ENSO by about one year. This dipole pattern of SLP anomalies is referred to as the NAD. We found that the NAD tends to be more closely related to the CP El Niño than the EP El Niño. In contrast, it appears that there is little difference in the relationship between the CP/EP El Niño and the PNA (or the NPO).

The present analysis presents a possible explanation of the processes by which the NAD can trigger the onset of CP El Niño events. Anomalous surface winds associated with the NAD can force a tripole-like SST pattern in the North Atlantic via changes in surface heat fluxes during spring. In particular, negative SST anomalies in the NTA can produce an anticyclonic flow over the subtropical northeastern Pacific by influencing the convective activity over the Atlantic ITCZ (Ham et al. 2013a), which in turn induces easterly anomalies in the eastern equatorial Pacific that cause the anomalous easterlies to dominate the eastern equatorial Pacific. Then, the anomalous convective activity along the Pacific ITCZ, due to the anomalous southerly flow on its west flank of this anticyclonic flow, produces a cyclonic flow over the western North Pacific during the JJA season. This cyclonic flow generates westerly anomalies in the western equatorial Pacific. The anomalous westerlies in the western equatorial Pacific, and the anomalous easterlies in the eastern equatorial Pacific, may cause convergence in the central equatorial Pacific, and in turn trigger the warming there. This warming gradually develops in the central equatorial Pacific through a local ocean–atmosphere coupling process, finally establishing a CP El Niño pattern in the tropical Pacific during the following winter. We suggest that the NTA SST may play an important role in linking the NAD to the CP El Niño, as has been documented by Ham et al. (2013a, b).

The NAD, PNA and NAO are related to one another because their related SLP anomalies overlap over some regions of the North America and western North Atlantic. However, there are in fact remarkable differences among them. In Fig. 15a we summarize the major differences among them. The NAD-related SLP anomalies are mainly located over northeastern North America to the western tropical North Atlantic, while the PNA-related SLP anomalies are mainly confined in the North Pacific basin and do not extend sufficiently into the western tropical North Atlantic. The SLP anomaly centre of the NAD is located further towards the NTA region than that of the NAO. As a result, the NAD tends to be more effective in forcing the NTA SST anomalies than does the PNA or the NAO (Fig. 15b), while the NTA SST anomalies have been shown to play an important role in developing subsequent CP El Niño events. Thus, the NAD variations contain more unique precursor information regarding the development of large-scale SST anomalies associated with CP El Niño events than do the PNA or the NAO.

The joint relationship of the NAD and NPO to the onset of CP El Niño events was also examined in this study. We found that the relationship of either the NAD index or the NPO index to the development of subsequent CP El Niño

events depends on the status of the other index. When the wintertime NAD index is of the opposite sign to the simultaneous NPO index, the correlation of the NAD or NPO index with the following CP El Niño state becomes much weaker. One possible reason for this correlation change is that the NAD influence on the tropical Pacific interferes with the NPO effect when the NAD and NPO indices are of the opposite sign. The joint role of the NAD and NPO in initiating the onset of CP El Niño events leads us to speculate that the NAD and NPO variations may together serve as a precursor to CP El Niño events. Further research is required to examine the real predictive use of the combined NAD and NPO precursor signals as a supplemental tool for prediction of the CP El Niño within a forecast framework.

It should be noted that, even though the observational analysis presented above highlights the potential importance of the NAD in contributing to the CP El Niño development through its influence on the NTA SST, it has limitations due to a mixture of various climate variabilities in the observational records. For example, because some NAD events accompany ENSO events, it is difficult to completely isolate the individual influence of the NAD-induced NTA SST anomalies on the CP El Niño events. Further work is required using a coupled general circulation model (CGCM) to examine to what extent the NAD → NTA SST → CP El Niño process can influence the CP El Niño. In addition, it is important to note that the lagged relationship between the NAD and CP El Niño is not stationary but has undergone a distinct decadal variation. Figure 16 shows the sliding correlation between the winter NAD index and the following winter Niño4 index for the period 1950–2013. The correlation is very weak in the 1960s and 1970s, but increases after the early 1980s, and reaches (and even exceeds) the 90 % confidence level from the 1990s onwards. Recent studies have noted that CP El Niño events have occurred more frequently than EP El Niño events since the 1990s (Lee and McPhaden 2010), which has been attributed to anthropogenically forced global warming (Yeh et al. 2009) or natural variability (McPhaden et al. 2011; Newman et al. 2011; Yu et al. 2015). It is unclear whether the strengthened influence of the NAD on the CP El Niño after the 1990s favors the frequent occurrence of CP El Niño events over this period. In addition, the underlying mechanisms responsible for the strengthened linkage between the NAD and the CP El Niño after the 1990s remain unexplained. The present analysis indicates that the NAD influence on subsequent CP El Niño events involves the joint role of the NPO. Yeh et al. (2015) indicated that the NPO-like atmospheric circulation becomes more effective at playing a role in initiating CP El Niño after 1990. It remains to be explained whether decadal changes in the relationship between the NAD/NPO and the CP El Niño are linked to a shift in the relationship between the NAD and NPO. Further study is required in this regard.

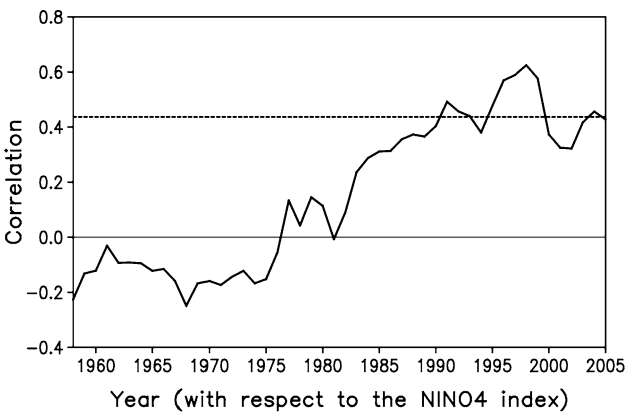

Fig. 16 The 15-year sliding correlation between the winter NAD index and the following winter Niño4 index for the period 1950–2013. The *horizontal dashed line* shows the 90 % confidence level

Acknowledgments This research was jointly supported by the China Special Fund for Meteorological Research in the Public Interest (GYHY201506013), the 973 project of China (2016YFA0601801), the National Natural Science Foundation of China for Excellent Young Scholars (41522502), and the Strategic Priority Research Program of the Chinese Academy of Sciences (XDA11010303).

References

Alexander MA, Vimont DJ, Chang P, Scott JD (2010) The impact of extratropical atmospheric variability on ENSO: testing the seasonal footprinting mechanism using coupled model experiments. J Clim 23:2885–2901

Anderson BT (2003) Tropical Pacific sea-surface temperatures and preceding sea level pressure anomalies in the subtropical North Pacific. J Geophys Res 108:D23. doi:10.1029/2003JD003805

Anderson BT (2007) On the joint role of subtropical atmospheric variability and equatorial subsurface heat content anomalies in initiating the onset of ENSO events. J Clim 20:1593–1599

Anderson BT, Perez RC, Karspeck A (2013) Triggering of El Niño onset through trade wind–induced charging of the equatorial Pacific. Geophys Res Lett 40:1212–1216. doi:10.1002/grl.50200

Ashok K, Yamagata T (2009) The El Niño with a difference. Nature 461:481–484

Ashok K, Behera SK, Rao SA, Weng YH, Yamagata T (2007) El Niño Modoki and its possible teleconnection. J Geophys Res 112:C11007. doi:10.1029/2006JC003798

Barnston AG, Livezey RE (1987) Classification, seasonality and persistence of low-frequency atmospheric circulation patterns. Mon Wea Rev 115:1083–1126

Bond NA, Overland JE, Spillane M, Stabeno P (2003) Recent shifts in the state of the North Pacific. Geophys Res Lett 30:2183. doi:10.1029/2003GL018597

Bretherton CS, Smith C, Wallace JM (1992) An intercomparison of methods for finding coupled patterns in climate data. J Clim 5:541–560

Capotondi A, Sardeshmukh PD (2015) Optimal precursors of different types of ENSO events. Geophys Res Lett 42:9952–9960. doi:10.1002/2015GL066171

Capotondi A et al (2015) Understanding ENSO Diversity. Bull Amer Meteor Soc 96:921–938
Cayan DR (1992) Latent and sensible heat flux anomalies over the northern oceans: driving the sea surface temperature. J Phys Oceanogr 22:859–881
Chang P, Zhang L, Saravanan R, Vimont DJ, Chiang JCH, Ji L, Seidel H, Tippett MK (2007) Pacific meridional mode and El Niño-Southern Oscillation. Geophys Res Lett 34:L16608. doi:10.1029/2007GL030302
Chiang J, Vimont DJ (2004) Analogous Pacific and Atlantic meridional modes of tropical atmosphere–ocean variability. J Clim 17:4143–4158
Deser C, Timlin M (1997) Atmosphere-ocean interaction on weekly timescales in the North Atlantic and Pacific. J Clim 10:393–408
Ding RQ, Li JP, Tseng YH, Sun C, Guo YP (2015a) The Victoria mode in the North Pacific linking extratropical sea level pressure variations to ENSO. J Geophys Res 120:27–45. doi:10.1002/2014JD022221
Ding RQ, Li JP, Tseng YH, Yuan CQ (2015b) Influence of the North Pacific Victoria mode on the Pacific ITCZ summer precipitation. J Geophys Res 120:964–979. doi:10.1002/2014JD022364
Feng J, Li JP (2011) Influence of El Niño Modoki on spring rainfall over South China. J Geophys Res 116:D13102. doi:10.1029/2010JD015160
Giese BS, Ray S (2011) El Niño variability in simple ocean data assimilation (SODA), 1871–2008. J Geophys Res 116:C02024. doi:10.1029/2010JC006695
Gushchina D, Dewitte B (2012) Intraseasonal tropical atmospheric variability associated with the two flavors of El Niño. Mon Wea Rev 140:3669–3681
Ham YG, Kug JS, Park JY, Jin FF (2013a) Sea surface temperature in the north tropical Atlantic as a trigger for El Niño/Southern Oscillation events. Nat Geosci 6:112–116
Ham YG, Kug JS, Park JY (2013b) Two distinct roles of Atlantic SSTs in ENSO variability: north Tropical Atlantic SST and Atlantic Niño. Geophys Res Lett 40:4012–4017. doi:10.1002/grl.50729
Horel JD, Wallace JM (1981) Planetary-scale atmospheric phenomena associated with the Southern Oscillation. Mon Wea Rev 109:813–829
Hurrell JW (1995) Decadal trends in the North Atlantic Oscillation: regional temperatures and precipitation. Science 269:676–679
Kalnay E et al (1996) The NCEP–NCAR 40-Year Reanalysis Project. Bull Amer Meteor Soc 77:437–471
Kao HY, Yu JY (2009) Contrasting eastern Pacific and central Pacific types of ENSO. J Clim 22:615–632
Kim ST, Yu JY, Kumar A, Wang H (2012) Examination of the two types of ENSO in the NCEP CFS model and its extratropical associations. Mon Wea Rev 140:1908–1923
Kug JS, Jin FF, An SI (2009) Two types of El Niño events: cold tongue El Niño and warm pool El Niño. J Clim 22:1499–1515
Larkin NK, Harrison DE (2005) Global seasonal temperature and precipitation anomalies during El Niño autumn and winter. Geophys Res Lett 32:L16705. doi:10.1029/2005GL022860
Larson SM, Kirtman BP (2014) The Pacific meridional mode as an ENSO precursor and predictor in the North American multimodel ensemble. J Clim 27:7018–7032
Lee T, McPhaden MJ (2010) Increasing intensity of El Niño in the central-equatorial Pacific. Geophys Res Lett 37:L14603. doi:10.1029/2010GL044007
Li JP, Wang JXL (2003) A new North Atlantic Oscillation index and its variability. Adv Atmos Sci 20:661–676
Lin CY, Yu JY, Hsu HH (2015) CMIP5 model simulations of the Pacific meridional mode and its connection to the two types of ENSO. Int J Climatol 35:2352–2358
Linkin ME, Nigam S (2008) The North Pacific oscillation-West Pacific teleconnection pattern: mature-phase structure and winter impacts. J Clim 21:1979–1997
Marshall J, Kushnir Y, Chang P, Battisti D, Czaja A, Dickson R, Hurrell J, McCartney M, Saravanan R, Visbeck M (2001) North Atlantic climate variability: phenomena, impacts, and mechanisms. Int J Climatol 21:1863–1898
McPhaden MJ, Lee T, McClurg D (2011) El Niño and its relationship to changing background conditions in the tropical Pacific Ocean. Geophys Res Lett 38:L15709. doi:10.1029/2011GL048275
Newman M, Shin SI, Alexander MA (2011) Natural variation in ENSO flavors. Geophys Res Lett 38:L14705. doi:10.1029/2011GL047658
Pan LL (2005) Observed positive feedback between the NAO and the North Atlantic SSTA tripole. Geophys Res Lett 32:L06707. doi:10.1029/2005GL022427
Pegion K, Alexander MA (2013) The seasonal footprinting mechanism in CFSv2: simulation and impact on ENSO prediction. Clim Dyn 41:1671–1683
Ren HL, Jin FF (2011) Niño indices for two types of ENSO. Geophys Res Lett 38:L04704. doi:10.1029/2010GL046031
Rogers JC (1981) The North Pacific Oscillation. J Climatol 1:39–57
Simmons AJ, Wallace JM, Branstator GW (1983) Barotropic wave propagation and instability, and atmospheric teleconnection patterns. J Atmos Sci 40:1363–1392
Smith TM, Reynolds RW, Peterson TC, Lawrimore J (2008) Improvements to NOAA's historical merged land-ocean surface temperature analysis (1880–2006). J Clim 21:2283–2296
Taschetto AS, England MH (2009) El Niño Modoki impacts on Australian rainfall. J Clim 22:3167–3174
Trenberth KE, Branstator GW, Karoly D, Kumar A, Lau N, Ropelewski C (1998) Progress during TOGA in understanding and modeling global teleconnections associated with tropical sea surface temperatures. J Geophys Res 103:14291–14324
Vimont DJ, Battisti DS, Hirst AC (2001) Footprinting: a seasonal connection between the tropics and mid-latitudes. Geophys Res Lett 28:3923–3926
Vimont DJ, Wallace JM, Battisti DS (2003a) The seasonal footprinting mechanism in the Pacific: implications for ENSO. J Clim 16:2668–2675
Vimont DJ, Battisti DS, Hirst AC (2003b) The seasonal footprinting mechanism in the CSIRO general circulation models. J Clim 16:2653–2667
Walker GT, Bliss EW (1932) World weather. V Mem Roy Meteor Soc 4:53–84
Wallace JM, Gutzler DS (1981) Teleconnections in the geopotential height field during the northern hemisphere winter. Mon Wea Rev 109:784–812
Weng HY, Wu XG, Liu YM, Behera SK, Yamagata T (2011) Anomalous summer climate in China influenced by the tropical Indo-Pacific Oceans. Clim Dyn 36:769–782
Wilson AB, Bromwich DH, Hines KM, Wang SH (2014) El Niño flavors and their simulated impacts on atmospheric circulation in the high southern latitudes. J Clim 27:8934–8955
Xie P, Arkin PA (1997) Global precipitation: a 17-year monthly analysis based on gauge observations, satellite estimates, and numerical model outputs. Bull Am Meteorol Soc 78:2539–2558
Xie SP, Philander SGH (1994) A coupled ocean–atmosphere model of relevance to the ITCZ in the eastern Pacific. Tellus 46A:340–350
Yeh SW, Kug JS, Dewitte B, Kwon MH, Kirtman BP, Jin FF (2009) El Niño in a changing climate. Nature 461:511–514
Yeh SW, Wang X, Wang CZ, Dewitte B (2015) On the relationship between the North Pacific climate variability and the central Pacific El Niño. J Clim 28:663–677

Yu JY, Kao HY (2007) Decadal changes of ENSO persistence barrier in SST and ocean heat content indices: 1958–2001. J Geophys Res 112:125–138

Yu JY, Kim ST (2010) Three evolution patterns of Central-Pacific El Niño. Geophys Res Lett 37:L08706. doi:10.1029/2010GL042810

Yu JY, Kim ST (2011) Relationships between extratropical sea level pressure variations and the central Pacific and eastern Pacific types of ENSO. J Clim 24:708–720

Yu JY, Kao HY, Lee T (2010) Subtropics-related interannual sea surface temperature variability in the central equatorial Pacific. J Clim 23:2869–2884

Yu JY, Lu MM, Kim ST (2012) A change in the relationship between tropical central Pacific SST variability and the extratropical atmosphere around 1990. Environ Res Lett 7:034025. doi:10.1088/1748-9326/7/3/034025

Yu JY, Kao PK, Paek H, Hsu HH, Hung CW, Lu MM, An SI (2015) Linking emergence of the central Pacific El Niño to the Atlantic multidecadal oscillation. J Clim 28:651–662

Zhang Y, Wallace JM, Iwasaka N (1996) Is climate variability over the North Pacific a linear response to ENSO? J Clim 9:1468–1478

Zhang WJ, Wang L, Xiang QB, Qi L, He HJ (2015) Impacts of two types of La Nina on the NAO during boreal winter. Clim Dyn 44:1351–1366